Effects of light doping on the vibrational modes of finite-length polyacetylene chains

Shi-jie Xie and Liang-mo Mei
Department of Physics, Shandong University, Jinan 250100, People's Republic of China
(Received 29 December 1992)

With a local site-impurity potential in the framework of the Su, Schrieffer, and Heeger (SSH) model, both the dopant dependence and the chain-length dependence of the vibrational modes related to charged solitons in a finite *trans*-polyacetylene chain have been studied. The numerical calculations showed that the well-known Goldstone mode will be pinned by the dopant potentials as well as by the chain ends. Two localized modes were found in the acoustic-frequency branch. The results are in agreement with the infrared-active vibrational modes also observed in lightly doped polyacetylene cases. A comparison with the photoexcitation measurements has been given.

I. INTRODUCTION

The intense infrared-activity absorption induced by charged solitons is due to the localized vibrational-phonon modes around the structural defect, which arise from the symmetrical vibrational modes (Raman-active modes), but are redshifted with respect to these Raman modes.[1] In *trans*-polyacetylene three doping-induced principal infrared-active vibrational (IRAV) modes have been observed and are located at 930, 1288, and 1370 cm^{-1}, respectively.[2–4] The intensities of the observed IRAV modes in *trans*-polyacetylene are proportional to the dopant concentration, but the locations of the modes are essentially independent of the dopant species. However, the IRAV mode at ~ 930 cm^{-1} was not observed in photoinduced-absorption experiments[5] (shown in Fig. 1). Thus it was believed that the dopant alone is responsible for this mode, and it was further assumed that this broad and intense absorption at ~ 930 cm^{-1} was the Goldstone mode shifted up from zero frequency by pinning due to the Coulomb binding of the charged ions to the charged solitons.[6–7]

Recently, Phillpot,[8] Harigaya,[9] and Stafström[10] *et al.* have investigated how impurities may affect the static lattice and electronic structures of conjugated polymers. They used the continuous (TLM) and discrete (SSH) models, and adopted site-impurity or bond-impurity models to describe the effects of the charged dopant ions. The calculations were performed from both in a closed ring (periodic boundary conditions) and in an open chain (fixed-end boundary conditions). They obtained new impurity electronic states at the band edges beside the soliton electronic state at the middle of the gap. The results showed the importance of the boundary conditions in a short chain.[10] In fact, a local impurity potential will break the original lattice symmetry of the polyacetylene system, which makes the degree of order decrease. A change in the number of the localized states is expected. In order to know whether there exist new localized vibrational modes in one-dimensional doped polyacetylene chains, in this paper we studied the dynamics of small amplitude excitations around a soliton in a finite-length *trans*-polyacetylene chain by considering the Coulomb effects of the dopant ions. The calculations were carried out both in a closed ring with periodic boundaries and in an open chain with free-end boundaries.

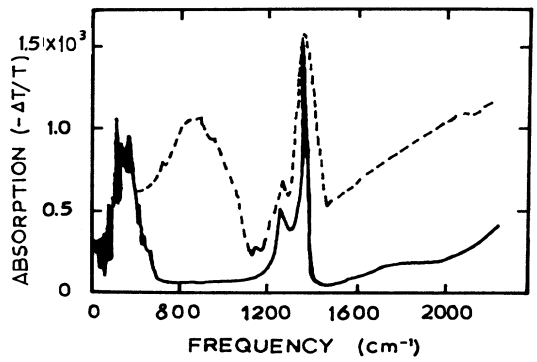

FIG. 1. Comparison of the infrared photoinduced (solid line) with doping-induced (dashed line) absorption spectra for *trans*-polyacetylene.

II. THE MODEL AND CALCULATION

The SSH model is generalized to include terms that describe Coulomb binding of charged solitons to the impurities. The Hamiltonian is given by

$$H = H_{\mathrm{SSH}} + H_{\mathrm{IMP}} \,. \tag{1}$$

The first term is the original SSH-model Hamiltonian[11]

$$H_{\mathrm{SSH}} = -\sum_{n,s} [t_0 - \alpha(u_{n+1} - u_n)] \times (C^{+}_{n+1,s} C_{n,s} + C^{+}_{n,s} C_{n+1,s}) + \frac{1}{2} K \sum_n (u_{n+1} - u_n)^2 + \frac{1}{2} M \sum_n \dot{u}_n^2 \,, \tag{2}$$

where t_0 is the nearest-neighbor hopping integral of the undimerized chain, α the electron-phonon coupling strength due to the modulation of the hopping integral, u_n the displacement of the nth (CH) unit, $C^{+}_{n,s}$ ($C_{n,s}$) the

creation (annihilation) operator of the π-electron with spin S at the nth site, K the force constant between adjacent units, and M the mass of (CH) unit. The dimensionless order parameter ϕ_n, the coupling λ, and the time τ were introduced as

$$\phi_n=(-1)^n\frac{\alpha}{t_0}u_n\ ,\quad \lambda=\frac{2\alpha^2}{\pi K t_0}\ ,\quad \tau=\omega_Q t\ , \tag{3}$$

where $\omega_Q=(4K/M)^{1/2}$ is the bare frequency. Then the SSH Hamiltonian will only depend on λ.

The second term of Eq. (1) represents effects of the impurity potential. A site-type form is adopted,[8]

$$H_{\rm IMP}=\sum_{m=1}^{N_i} V_d C^+_{m,s}C_{m,s}\ , \tag{4}$$

where m is the dopant ion position which is next to the lattice site, N_i the number of the dopant ions per chain, which gives the doping concentration ($y=N_i/N$), and V_d the interaction strength of the π electron with the dopant ion. Here we have omitted the dynamics of the dopant ion because of its mass which is heavier than that of the (CH) unit.

With a small deviation from the equilibrium configuration ϕ_n, the static condition and vibrational matrix can be derived by minimizing the total energy of the system.

A. A closed ring

For a closed ring, a periodic boundary condition was imposed on both the electronic and lattice systems in order to remove end-point effects, i.e.,

$$Z_{\mu,n+N,s}=Z_{\mu,n,s}\ ;\quad u_{n+N}=u_n\ . \tag{5}$$

The following formulas[12,13] were derived:

$$\phi_n+\phi_{n+1}=(-1)^n\pi\lambda\left[\sum_\mu{}' Z_{\mu,n}Z_{\mu,n+1}-\frac{1}{N}\sum_{\mu,n}{}' Z_{\mu,n}Z_{\mu,n+1}\right]\ , \tag{6}$$

$$B_{m,n}=\frac{2}{\pi\lambda}(\delta_{m,n-1}+2\delta_{m,n}+\delta_{m,n+1})+2(-1)^{m+n}\sum_\mu{}'\sum_{\nu(\neq\mu)}\frac{C^m_{\mu\nu}C^n_{\mu\nu}}{\epsilon_\mu-\epsilon_\nu}\ , \tag{7}$$

with $C^m_{\mu\nu}=Z_{\mu,m}\ (Z_{\nu,m+1}-Z_{\nu,m-1})+Z_{\nu,m}(Z_{\mu,m+1}-Z_{\mu,m-1})$. The spin symbol S was omitted. $B_{m,n}$ represents the vibrational matrix elements. Its eigenvalues and eigenstates of the vibrational matrix are the phonon frequencies and vibrational modes, respectively. Here ϵ_μ and $Z_{\mu,m}$ are the eigenvalue and eigenstate of electrons. They are determined by the following eigenequation:

$$-[1+(-1)^n(\phi_n+\phi_{n+1})]Z_{\mu,n+1}-[1+(-1)^{n-1}(\phi_{n-1}+\phi_n)]Z_{\mu,n-1}+\sum_m^{N_i}V_d\delta_{m,n}Z_{\mu,n}=\epsilon_\mu Z_{\mu,n}\ . \tag{8}$$

B. An open chain

For an open chain, a free-end boundary condition was assumed. In this case, an extra constraint must be applied to stabilize the system,

$$H'=K'\sum_n^{N-1}(u_{n+1}-u_n)\ , \tag{9}$$

where $K'=-4\alpha/\pi$ (Ref. 11).

In the same way, the static condition and the vibrational matrix in an open chain can be derived.

$$\phi_n+\phi_{n+1}=(-1)^n\pi\lambda\left[\sum_\mu{}' Z_{\mu,n}Z_{\mu,n+1}-\frac{2}{\pi}\right]\ , \tag{10}$$

$$B_{m,n}=\frac{2}{\pi\lambda}[(\delta_{m,n}+\delta_{m,n+1})(1-\delta_{m,N})+(\delta_{m,n}+\delta_{m,n-1})(1-\delta_{m,1})]+2(-1)^{m+n}\sum_\mu{}'\sum_{\nu(\neq\mu)}\frac{C^m_{\mu\nu}C^n_{\mu\nu}}{\epsilon_\mu-\epsilon_\nu}\ , \tag{11}$$

with

$$C^m_{\mu,\nu}=(1-\delta_{m,N})(Z_{\mu,m+1}Z_{\nu m}+Z_{\mu,m}Z_{\nu,m+1})-(1-\delta_{m,1})(Z_{\mu,m}Z_{\nu,m-1}+Z_{\mu,m-1}Z_{\nu,m})\ .$$

Here ϵ_μ and $Z_{\mu,m}$ are the eigenvalue and eigenstate of electrons in an open chain, respectively. They are determined by the following eigenequation:

$$-[1+(-1)^n(\phi_n+\phi_{n+1})](1-\delta_{n,N})Z_{\mu,n+1}-[1+(-1)^{n-1}(\phi_{n-1}+\phi_n)](1-\delta_{n,1})Z_{\mu,n-1}+\sum_m^{N_i}V_d\delta_{m,n}Z_{\mu,n}=\epsilon_\mu Z_{\mu,n}\ , \tag{12}$$

where $\delta_{i,j}$ is the Kroniker δ function

$$\delta_{i,j}=\begin{cases}1 & i=j\\ 0 & i\neq j\end{cases}\ . \tag{13}$$

Equations (6) and (8), and (10) and (12) were solved by numerical iteration for a closed ring and an open chain, respectively. The equilibrium bond configuration $\phi_n+\phi_{n+1}$ of the ring (or chain) with N_i site impurities can be easily obtained. Then by substituting it into Eq. (7) or Eq. (11) and diagonalizing $B_{m,n}$, all the vibrational models can be obtained, the localized ones can be picked out from these modes.

Numerical investigations were performed with the parameters of *trans*-polyacetylene $t_0=2.5$ ev, $\alpha=4.2$ ev/Å, and $K=18.7$ ev/Å^2. The dimensionless electron-phonon coupling constant $\lambda=0.24$ and $\omega=(8\lambda)^{1/2}\omega_0=1400$ cm^{-1} (phonon frequency at $k=0$) were obtained. An impurity site is located next to one of the total N lattice points. The convergence criterion is that the ith $|\phi_n+\phi_{n+1}|$ minus the $(i-1)$th $|\phi_n+\phi_{n+1}|$ is less than 10^{-5} for each n.

A negatively or positively charged soliton is eventually

produced for a donor (or acceptor) dopant with different Coulomb strength both in an odd-number ring and open chain. For an open chain, it is energetically favorable for the dopant ion to be at the center of the chain. For a closed ring, however, the system is energetically stable for any site position where the ion is doped, because of the translation symmetry along its chain. The static bond configuration $\phi_n+\phi_{n+1}$ in the impurity-free ($V_d=0$, dash line) and in the doped $V_d=-0.4t_0$, solid line) soliton-lattice systems are shown in Fig. 2(a). Figure 2(b) gives the energy band and the corresponding localized electronic states in a closed ring with a dopant potential $V_d=-0.4t_0$. A similar band structure has been obtained in an open chain.

Due to the attractive dopant potential, the soliton in the doped case becomes more localized, compared with the impurity-free case. For an open chain, an obvious characteristic is that an oscillation occurs in the bond configurations and is even stronger at the ends of the chain. Thus results from the breaking of bond symmetry at the chain ends. As the electron-hole symmetry is broken by the dopant, the soliton energy level deviates from the middle of the gap. In addition, a shallow energy level emerges at the bottom of the VB for the donor or at the top of the CB for the acceptor as shown in Fig. 2(b).

Further, the vibrational modes have been calculated. In the discrete lattice model (SSH) used here, calculations were performed on a chain consisting of 101 lattice sites. The number of extended modes were found to be 50 in the acoustic branch and 47 (with a weak localized mode g_4) in the optical branch for the undoped system. The first three of the five localized modes (g_1, g_2, g_3, g_s, and g_4) are purely optical and g_s is half optical and half acoustic. g_4 is the lowest optical frequency mode; its localization is very weak and depends upon the strength of electron-lattice coupling and the boundary conditions. For the doped system, the number of extended modes in

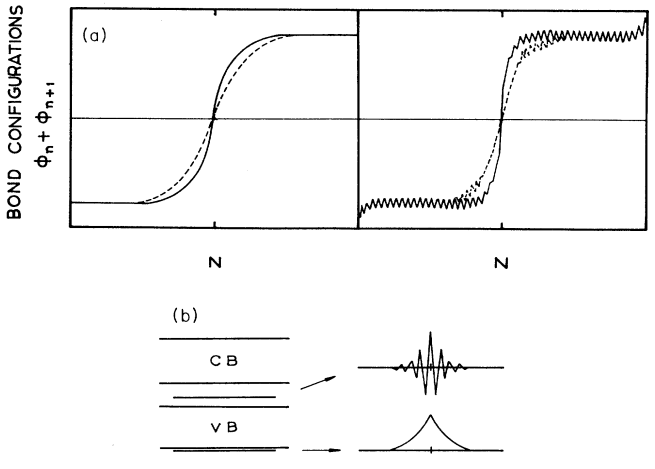

FIG. 2. Static characteristics of a site-doped polyacetylene chain: (a) Bond configuration $\phi_n+\phi_{n+1}$ in $V_d=0$ (dashed line) and $V_d=-0.4t_0$ (solid line); (b) energy band and localized electronic states ($V_d=-0.4t_0$).

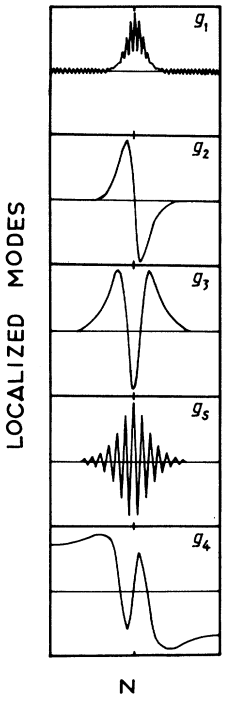

FIG. 3. Configurations of the localized modes in the impurity-free case ($V_d=0$).

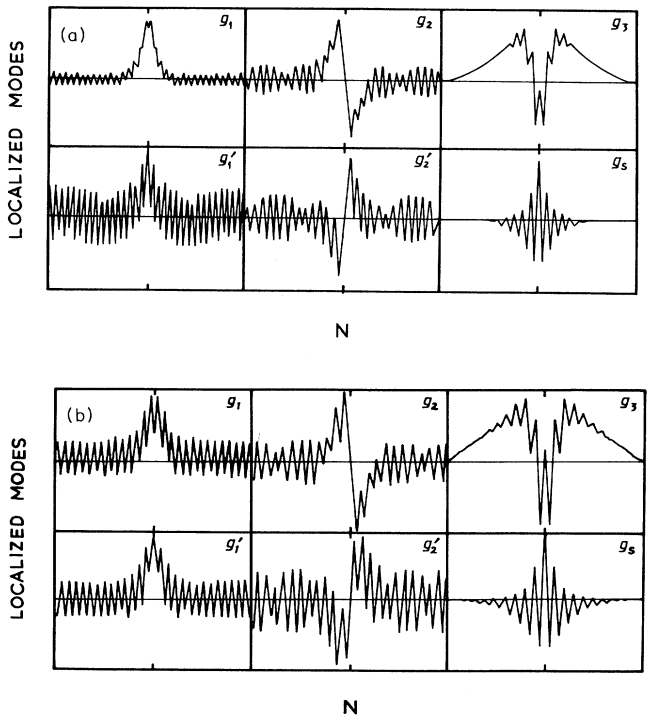

FIG. 4. Configurations of the localized modes in the doped case ($V_d=-0.4t_0$) with (a) periodic boundary condition or (b) natural boundary condition.

TABLE I. Frequency dependence of mode g_1 on the chain length in the natural boundary condition (ω/ω_0).

$L(C)$	13	17	21	25	41	81	∞	Exp.
g_1	0.523	0.393	0.291	0.217	0.001	$<10^{-4}$	0	0.393

the optical branch was found to still be 47, but in the acoustic branch, the number becomes less (48) due to the emergence of two new localized modes g_1' and g_2'. Compared with the localized models in the impurity-free-case, the intensity of the localized optical modes becomes weak as shown in Figs. 3 and 4. But the calculations show that some extended modes around (g_1,g_1') or (g_2,g_2') have a little sign of localization. We infer that the number of the localized modes around (g_1,g_1') or (g_2,g_2') might be varied with the potential strength of the dopant ion. Such changing of the number of extended (or localized) modes should be attributed to the breaking of the local symmetry in the chain by the dopants.

The chain-length dependence of the five localized modes obtained in the impurity-free soliton lattice system has been studied. The calculated results showed that the three infrared-active modes, g_1, g_3, and g_s, exhibit different behaviors. In a short open chain, the frequency of the mode g_1 shifts from zero to a finite value due to the breaking of the translation symmetry at the ends. When the chain length is $17C$ (C is the undimerized lattice constant), the frequency of mode g_1 is calculated to be 550 cm^{-1} (shown in Table I). This value is in good agreement with the experimental result. A similar result has been given with a molecular-orbital method.[16] Recently, Kim[14] and Mulazzi[15] have also predicated that the photoinduced IRAV mode at 500 cm^{-1} exhibits a more or less pronounced structured shape depending on the segments of different length contained in samples. Here, the end boundaries pin the Goldstone mode. The Goldstone theorem still holds, provided the chain is long enough ($>81C$). Modes g_3 and g_s do not change much with the chain length. Mode g_2, however, becomes extended at a very short chain length, and mode g_4 is always extended in the open chain no matter how long the chain is.

In the doped soliton lattice system, the calculations give four IRAV modes, two of which are modes g_3 and g_s, the third is the Goldstone mode g_1 which has been pinned by the local dopant potential and the last is a new even-parity mode g_1', which results from the dopant. Some properties of the localized modes are listed in Table II. One can see that the frequencies of modes g_1 and g_1' are close to one another. $V_d=-0.4t_0$, we obtained $\omega_1=929$ cm^{-1} and $\omega_1'=943$ cm^{-1} in a closed ring, and $\omega_1=922$ cm^{-1} and $\omega_1'=946$ cm^{-1} in an open chain. These data are in good agreement with the experimental observations (~ 930 cm^{-1}) in the doping-induced studies carried out on polyacetylene with dilute doping concentrations.[2-4] We can see from Fig. 1 that the IRAV peak at ~ 930 cm^{-1} is very broad, so it might consist of many couplies of g_1 and g_1'-like modes, since in real polyacetylene material the potential V_d is not a constant, but has a distribution.

The dopant potential has little influence on modes g_3 and g_s, as the data in Table II show. The frequency of g_3 increases slightly with the strength of V_d, and for g_s, the situation is the opposite. At $V_d=-0.4t_0$, the calculations give $\omega_3=1347$ cm^{-1} and $\omega_s=1335$ cm^{-1} in a closed ring, and $\omega_3=1354$ and cm^{-1} $\omega_s=1334$ cm^{-1} in an open chain. These results can explain the other two observed peaks in Fig. 1.

The calculations also give two non-IRAV modes, one of which is the second modes g_2, which has been weakly pinned by the dopant potential; the other is a new odd-parity mode g_2' resulting from the dopant. The frequency of both is close to one another. The weak localized mode g_4 found in the impurity-free system (periodic boundary conditions) becomes extended when the dopant effect is considered whether in an open chain or in a closed ring. These three are inversion symmetric (odd parity) and are not IR active.

In order to get a more general conclusion, we extended the dopant potential to a screening Coulomb form,[17]

TABLE II. Frequency dependence of the localized modes on the dopant potential V_d, both in a closed ring (C.R.) and in an open chain (O.P.).

		Frequency (ω/ω_0)						
		$V_d=0$		$V_d=-0.2t_0$		$V_d=-0.4t_0$		
Mode	Parity	C.R.	O.C.	C.R.	O.C.	C.R.	O.C.	Exp.
g_1	even	0	0	0.473	0.468	0.664	0.659	0.663
g_1'				0.485	0.485	0.674	0.676	
g_2	odd	0.802	0.805	0.824	0.830	0.852	0.867	
g_2'				0.831	0.836	0.864	0.877	
g_3	even	0.925	0.929	0.946	0.950	0.962	0.967	0.979
g_s	even	0.960	0.959	0.958	0.958	0.954	0.953	0.920
g_4	odd	0.963						

TABLE III. Frequency dependence of the localized modes on the screening factor β in a closed ring (ω/ω_0).

β	0.1	0.5	1.0	4.0
g_1	0.751	0.710	0.688	0.665
g_1'	0.758	0.721	0.695	0.675
g_2	0.886	0.871	0.867	0.852
g_2'	0.898	0.882	0.881	0.865
g_3	0.970	0.964	0.963	0.963
g_s	0.951	0.952	0.953	0.954

$$H_{\mathrm{IMP}}=\sum_{m,n} V_m(n)C_{n,s}^{+}C_{n,s} \ , \tag{14}$$

where

$$V_m(n)=\pm\frac{e^2}{\epsilon_\perp[(n-m)^2C^2+(\epsilon_\parallel/\epsilon_\perp)d^2]^{1/2}} \times\exp[-\beta|n-m|] \tag{15}$$

is the interaction between electrons on site n and the dopant side by site m of the chain, e is the magnitude of the unit charger, $\epsilon_\perp$ and $\epsilon_\parallel$ represent the dielectric constant perpendicular and parallel directions to the chain respectively, C is the lattice constant of the undimerized system, d is the perpendicular distance between the chain and the dopant ion, and β represents the potential screening along the chain. "+" is taken for an acceptor and "−" for a donor.

Calculations were performed with $\epsilon_\perp=10.0$ and $\epsilon_\parallel=3.5$ to obtain the vibrational-phonon modes in a negatively charged soliton lattice system. Other parameters in Eq. (15) are $C=1.22$ Å, $d=2.4$ Å, and $e^2=14.3$ ev/Å. With the same convergence criterion, we obtained the localized modes for different screening factors, β. The frequencies calculated for a closed ring with a site-type screening Coulomb potential for all localized modes are listed in Table III. We can see that the frequencies change little with the interaction screening factor β in the range 0.1–4.0. This indicates that the main results do not depend on whether the impurity potentials are short or long ranged. A similar conclusion is obtained in an open chain case.

III. CONCLUSIONS

In the present paper we have numerically investigated the lattice configurations, electronic energy structures, and localized phonon modes of the charged soliton by considering the short-range and long-range site-type dopant potential in the framework of the SSH model. A comparison with IRAV observations on dilute doped *trans*-polyacetylene has been made. The calculations presented both in a closed ring and in an open chain showed that the boundary conditions are not important to the localized modes if the chain is long enough. But in a short chain, the translation mode g_1 will be pinned by the chain ends. This leads to the moving up of the frequency of mode g_1. The local dopant potential breaks the original symmetry of the chain, making the degree of order of the system lower. It cannot only affect the soliton states, introduce impurity states away from the band edges, but also affect the phonon spectrum and the vibrational modes. The intensities and frequencies of the g_1, g_2, and g_4 modes of charged solitons will be changed to some extent due to the Coulomb binding of the dopant ion. The even-parity modes g_3 and g_s both are intrinsic modes and are slightly dependent on the dopants. The most important point is that two new localized modes (g_1' and g_2') have first been shown to exist in the acoustic branch in doping cases. These conclusions are independent of the choice of the boundary condition as long as the chain is long enough compared with the soliton width. The results have shown the importance of the doping effect.

ACKNOWLEDGMENT

The authors thank Professor X. Sun for fruitful discussions.

[1]A. J. Heeger, S. Kivelson, J. R. Schrieffer, and W. P. Su, Rev. Mod. Phys. **60**, 781 (1988).
[2]C. R. Fincher, M. Ozaki, A. J. Heeger, and A. G. MacDiarmid, Phys. Rev. B **19**, 4140 (1979).
[3]J. F. Rabolt, T. C. Clarke, and G. B. Street, J. Chem. Phys. **71**, 4614 (1979).
[4]S. Etemad *et al.*, Phys. Rev. B **23**, 5137 (1981).
[5]Z. Vardeny *et al.*, Phys. Rev. Lett. **50**, 2023 (1983); G. Blanchet *et al.*, *ibid.* **50**, 1938 (1983).
[6]J. C. Hicks and J. T. Gammel, Phys. Rev. B **37**, 6315 (1988).
[7]R. J. Cohen and A. J. Glick, Phys. Rev. B **36**, 2907 (1987).
[8]S. R. Phillpot, D. Baeriswyl, A. R. Bishop, and P. S. Lomdahl, Phys. Rev. B **35**, 7533 (1987).
[9]K. Harigaya, Y. Wada, and F. Fesser, Phys. Rev. Lett. **63**, 2401 (1989); Phys. Rev. B **42**, 1268 (1990).
[10]S. Stafström, Phys. Rev. B **43**, 9158 (1991).
[11]W. P. Su, J. R. Schrieffer, and A. J. Heeger, Phys. Rev. Lett. **42**, 1698 (1979); Phys. Rev. B **22**, 2099 (1980).
[12]X. Sun, C. Wu, and X. Shen, Solid State. Commun. **56**, 1039 (1985); Phys. Rev. B **35**, 4102 (1987).
[13]X. Sun, C. Wu, R. Fu, S. Xie, and K. Nasu, Phys. Rev. B **35**, 4102 (1987).
[14]Y. H. Kim and A. J. Heeger, Phys. Rev. B **40**, 8393 (1989).
[15]E. Mulazzi and A. Ripamonti, Phys. Rev. B **45**, 9439 (1992).
[16]Y. Mori and S. Kuirhara, Solid State Commun. **64**, 947 (1987).
[17]W. Bryant and A. J. Glick, Phys. Rev. B **26**, 5855 (1982); S. Tabor and S. Stafström, *ibid.* **44**, 12 737 (1991).